A. R. Kumar
Department of Mechanical Engineering,
University of Florida,
Gainesville, FL 32611

V. A. Boychev
Department of Physics,
University of Florida,
Gainesville, FL 32611

Z. M. Zhang[1]
Department of Mechanical Engineering,
University of Florida,
Gainseville, FL 32611
e-mail: zzhang@cimar.me.ufl.edu

D. B. Tanner
Department of Physics,
University of Florida,
Gainesville, FL 32611

Fabry-Perot Resonators Built With $YBa_2Cu_3O_{7-\delta}$ Films on Si Substrates

Fabry-Perot resonators were built from two superconductive $YBa_2Cu_3O_{7-\delta}$ (YBCO) films separated by a spacer. Each film of 35-nm thickness was deposited on a Si substrate, about 204 μm thick. A slow-scan Michelson interferometer was employed to measure the transmittance of the resonator in the far-infrared frequency region from 10 to 90 cm^{-1} at temperatures between 10 and 300 K. Measurements showed that in the normal state the peak (or resonant) transmittance decreases as temperature is lowered, whereas in the superconducting state it can increase with decreasing temperature. The transmittance of the resonator was calculated using properties of individual reflectors obtained previously. When the effect of partial coherence is taken into consideration, the calculated transmittance is in good agreement with the experiments. Furthermore, the maximum possible resonant transmittance was predicted based on an optimization analysis in which the cavity length is varied. The effect of the YBCO film thickness on the transmittance peaks was also studied, showing that the resonant transmittance decreases but the finesse increases as the film thickness is increased. This study should help improve the future design of Fabry-Perot resonators based on HTSC thin films. [S0022-1481(00)00604-6]

1 Introduction

Observations in the far-infrared region play an important role in the fields of astrophysics, chemical analysis, and molecular spectroscopy. Far-infrared studies in astrophysics include the cooling lines of star forming regions, associated cold dust, and spectra of giant planets ([1]). The pure rotational spectra of molecules and absorption bands in solids and liquids generally fall in the far-infrared region. Most of these studies require high precision measurements of the far-infrared radiation in a very narrow band; this can be achieved with the help of Fabry-Perot resonators ([2]). Fabry-Perot resonators can also be used as adaptable interferometers and in laser-line analysis ([2,3]). A simple resonator consists of two reflecting mirrors facing each other separated by a medium that is usually air or vacuum or a gas which needs to be analyzed. The most commonly employed reflectors in the far-infrared region are metallic meshes ([4,5]).

High-temperature superconducting (HTSC) thin films on transparent substrates have been considered as a potential substitute for the metallic mesh reflectors in far-infrared resonators ([6]). Metallic meshes show absorption at infrared frequencies due to the ohmic losses from the current induced in the wires ([5]). This absorption within the metallic mesh limits the finesse of the resonators. In the superconducting state, the thin films have no ohmic losses (i.e., no absorption) for frequencies up to their superconducting energy gap, which lies in the far-infrared region for HTSC materials. Hence, Fabry-Perot resonators built with HTSC thin films should offer a higher finesse than those with metallic meshes, although some residual absorption still exists at low temperatures due to noncondensing electrons. Another advantage is the suppression of high-frequency radiation, as HTSC materials are more opaque than the metallic-mesh at high frequencies.

Renk et al. [6] reported the use of HTSC thin films for the construction of far-infrared resonators in the frequency range up to 300 cm^{-1}. They used 100-nm-thick YBCO films on 1-mm thick MgO substrates as reflectors and a cavity length of 44 μm. The obtained peak transmittance was 0.016 with a finesse $F=30$ for the first-order resonance. The lower transmittance was due to the relatively thick YBCO film. Wiese et al. [7] measured the transmittance of a resonator made from two reflectors: a 50-nm-thick YBCO film on a 0.35-mm-thick MgO substrate and a 70-nm-thick film on a 0.25-mm-thick MgO substrate. The reported peak transmittance was 0.16 and $F=55$ for the first-order resonance located near 80 cm^{-1}. In order to obtain a high peak transmittance, the HTSC films should be thin enough so that the transmittance will not be too low and the substrates should effectively transmit in the frequency region of interest. Pechen et al. [8] measured the transmittance of a resonator built from 30-nm-thick YBCO films deposited on 0.5-mm-thick Si substrates. The measured peak transmittance at 10 K was about 0.6 with $F=20$ at the first-order resonance frequency of 60 cm^{-1}. Although this peak transmittance is much higher than that obtained in the previous studies, the resonance in the substrates has caused strong sidebands that overlap the main resonance peaks.

In the present paper, we describe the transmittance measurement of resonators built from two reflectors, each consisting of a 35-nm-thick YBCO film deposited on a Si substrate (about 204 μm thick). Measurements were carried out in the frequency region from 10 to 90 cm^{-1} at fixed temperatures between 10 and 300 K. The smaller thickness of the substrate used in the current work allows the distinction of the main resonance from the sidebands caused by interference effects in the substrates. In addition, the optimum cavity length that results in maximum peak transmittance was computed by coupling the cavity resonance with the resonance in the substrate. The effect of the YBCO film thickness on the peak transmittance of the resonator was also studied.

2 Theoretical Background

A simple plane Fabry-Perot resonator consists of two parallel mirrors separated by a gap, with their reflecting surfaces facing each other. In the present experiments, two Si substrates coated with YBCO films were used to form a resonator as shown in Fig. 1(*a*). The transmittance through this multilayer structure was derived using the two-effective-interface method. The transmittance of the resonator is ([2])

[1]To whom correspondence should be addressed.

Contributed by the Heat Transfer Division for publication in the JOURNAL OF HEAT TRANSFER and presented at the 1999 IMECE, Nashville, TN. Manuscript received by the Heat Transfer Division, July 9, 1999; revision received, May 25, 2000. Associate Technical Editor: D. Poulikakos.

$$\mathcal{T}=\frac{\dfrac{T_1T_2}{(1-\sqrt{R_1R_2})^2}}{1+\dfrac{4\sqrt{R_1R_2}}{(1-\sqrt{R_1R_2})^2}\sin^2\left(\dfrac{\beta+\phi_1+\phi_2}{2}\right)} \tag{1}$$

where subscripts 1 and 2 indicate the first and the second film/substrate composite, T and R are the transmittance and the film-side reflectance of the composite, $\beta=4\pi\omega d$ is the phase shift of the radiation at frequency ω (in cm^{-1}) for one round trip inside the cavity of length d (in cm) with a refractive index equal to 1, and ϕ is the phase shift upon refection at the film surface. Equation (1) can be expressed in a more compact form using the definitions of finesse,

$$F=\frac{\pi(R_1R_2)^{1/4}}{1-\sqrt{R_1R_2}}, \tag{2}$$

and resonant transmittance,

$$\mathcal{T}_{\text{res}}=\frac{T_1T_2}{(1-\sqrt{R_1R_2})^2}. \tag{3}$$

Hence, the transmittance of the resonator is

$$\mathcal{T}=\frac{\mathcal{T}_{\text{res}}}{1+\dfrac{4F^2}{\pi_2}\sin^2\left(\dfrac{\psi}{2}\right)} \tag{4}$$

where $\psi=\beta+\phi_1+\phi_2$. The transmittance reaches its maxima ($\mathcal{T}_{\text{res}}$) for $\psi=2m\pi$ and its minima for $\psi=(2m+1)\pi$ where m is the order of the interference fringe. If the change in $\mathcal{T}_{\text{res}}$ is small, for locations of the half maxima can be calculated by setting the denominator in Eq. (4) to be 2, i.e., $F^2\sin^2(\psi/2)=\pi^2/4$. For large values of F, $\psi=2m\pi\pm\pi/F$. If changes in ϕ_1 and ϕ_2 are neglected, the full-width-at-half-maximum (FWHM) bandwidth is $(2dF)^{-1}$. This is consistent with the definition of finesse F, which is the ratio of fringe separation or free spectral range, $\Delta\omega=(2d)^{-1}$, to the FWHM bandwidth. For a given cavity length, F is inversely proportional to the bandwidth of the transmittance peak. The effects of interference inside the substrate are included in the T and R terms, which can cause additional oscillations (sidebands) in the transmittance spectra and/or interfere with the resonant transmittance peaks. Hence, the actual bandwidth and finesse may differ significantly from the simplified calculations. It is noteworthy that the transmittance of the resonator can also be calculated using the transfer-matrix method ([9,10]). Because Eqs. (2)–(4) clearly distinguish the influence of the cavity resonance from the properties of each individual reflector, they are employed in the present analysis.

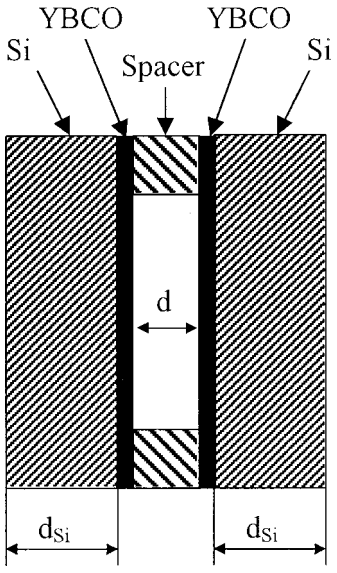

Fig. 1 The cross-sectional view of the resonator structure (not to scale)

3 Experiments

In the present study, each reflecting surface was made of a 35-nm-thick YBCO film deposited on a 12 mm × 12 mm Si substrate of 204 μm (±1 μm) thickness. The superconductive films were deposited at the National Institute of Standards and Technology by a laser ablation technique using yttria-stabilized zirconia and CeO_2 buffer layers ([11,12]). The YBCO films were *a-b* plane oriented with a critical temperature (T_c) between 80 and 82 K. The spacer that separates the two films was either a polyimide sheet of 132-μm thickness or a copper plate of 550-μm thickness, with a hole at the center. The cross-sectional view of the resonator arrangement is shown in Fig. 1. The distance between the two films, i.e., the cavity length d, is determined by the spacer.

Two identical copper plates with equally sized apertures (6 mm in diameter) were mounted at a right angle on the sample holder; one is used to mount the resonator structure and the other is left blank for reference measurements, as shown in Fig. 2. Slightly curved beryllium copper strips (2 mm wide, 0.2 mm thick, and 5 mm long), fastened with screws on the corners of one plate, acted like springs (due to their high elasticity) to hold the films along with the spacer to the copper plate. This sample holder was mounted on the cold finger inside the cryostat. The cold finger was kept in high vacuum and cooled by liquid helium, resulting in conductive cooling of the films. The transmittance spectra were measured using a slow-scan Michelson interferometer with a mercury-arc lamp source and a liquid-helium-cooled silicon bolometer. The construction details of this particular interferometer were reported by Sanderson and Scott [13]. The transmittance spectra of individual films were measured with the same experimental arrangements and analyzed to obtain the dielectric function of individual films at various temperatures ([12]).

The transmittance of the resonator structure was measured at temperatures of 10, 50, 100, 200, and 300 K in the frequency region from 10 to 90 cm^{-1}. The measured transmittance spectra for the resonator with a polyimide spacer are shown in Fig. 3. The transmittance peaks resulting from the resonance within the cavity are located at $\omega_m=m/2d$, where $m=1,2,\ldots$. Therefore, the transmittance peaks of the first and second-order resonance for this spacer are approximately located at 39 cm^{-1} and 76 cm^{-1}, respectively. The actual resonance frequency are determined by ψ, which is influenced by ϕ_1 and ϕ_2. The resonant transmittance

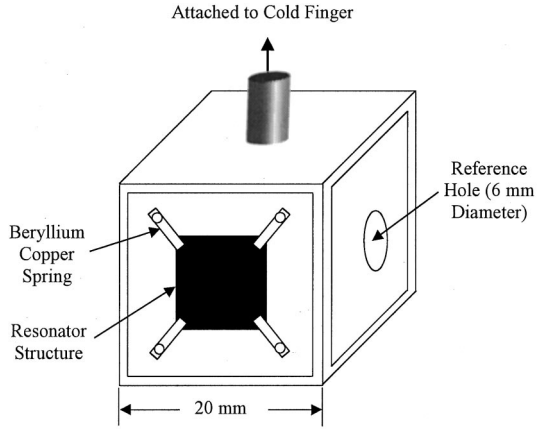

Fig. 2 Schematic of the sample holder

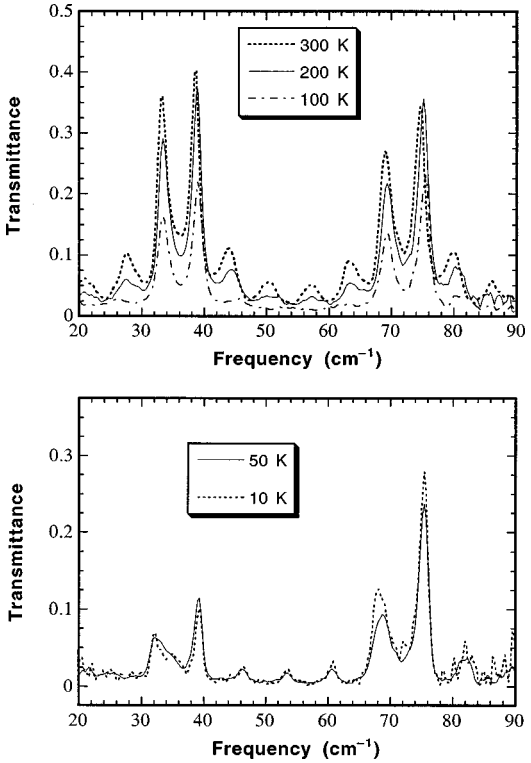

Fig. 3 Measured transmittance of the Fabry-Perot resonator with the polyimide spacer at various temperatures

peaks are shifted toward higher frequencies as the temperature is lowered. This can be explained by the decrease in the refractive index of the Si substrate as the temperature is lowered. The resonance (or interference) within the Si substrates is coupled to the main resonance inside the cavity, resulting in complex fringes. The sidebands include additional transmittance peaks near the main resonance and ripples in the spectra.

Above 100 K the peak transmittance associated with sidebands is comparable to that of the main resonance. In the normal state $\mathcal{T}_{\rm res}$ decreases with temperature, by a factor of two from 300 to 100 K. If both the YBCO films were identical, then $\mathcal{T}_{\rm res}$ given by Eq. (3) is reduced to ([4])

$$\mathcal{T}_{\rm res}=\frac{1}{(1+A/T)^2} \tag{5}$$

where $A=1-T-R$ is the absorptance of the film/substrate composite. The smaller the value of A/T, the higher the resonant transmittance $\mathcal{T}_{\rm res}$. The YBCO material exhibits a metallic behavior in the normal state. Its electrical conductivity will increase as the temperature decreases, yielding a reduction in the transmittance and an increase in the reflectance. The absorptance for radiation incident on the film side does not change significantly with temperature in the normal state ([14]). Therefore, as the temperature is lowered, the resonant transmittance decreases whereas the finesse increases, which means a decrease in the bandwidth. The transmittance associated with the sidebands shows a relatively higher percentage of reduction than the main resonant transmittance, because the increase in the reflectance of the YBCO films has suppressed the interference effects within the Si substrates.

In the superconducting state, the sidebands are suppressed even more significantly in comparison with the main resonance and this difference becomes larger at the second-order resonance. Another feature associated with the superconducting state is that at some frequencies, the peak transmittance increases as the temperature is lowered. This is particularly true at the second-order resonance (76 cm^{-1}), where $\mathcal{T}_{\rm res}$ is increased from 0.24 at 50 K to 0.28 at 10 K. Similar behavior was observed in the transmittance spectra of a single film/substrate composite due to the resonance in the Si substrate ([12]). The radiative properties of YBCO in the superconducting state differ greatly from those in the normal state. In the superconducting state, HTSC materials tend to show perfect reflection and little absorption for radiation at frequencies up to the energy gap. Decreasing the temperature causes an increase in the fraction of superconducting electrons and a decrease in the far-infrared absorptance ([15]). Hence, the increase in the peak transmittance from 50 K to 10 K can be attributed to the decrease in the absorptance within the YBCO films. Similar to the normal state, the bandwidth also decreases with the decrease in temperature, because of the increase in the reflectance. The measured finesse at 76 cm^{-1} is approximately 20 at 50 K and 23 at 10 K.

4 Calculation and Comparison

The transmittance T, film-side reflectance R, and phase shift ϕ of each reflector can be calculated using the optical constants of the film and substrate, assuming it is composed of a thin absorbing film on a thin (coherent) transparent substrate ([14]). There exists a large difference between the film-side reflectance and the backside reflectance ([16]). Calculation of the transmittance and reflectance requires prior knowledge of the frequency-dependent dielectric function of the thin-film materials. The dielectric function of YBCO in the far-infrared region is computed using the Drude model in the normal state and a two-fluid model in the superconducting state ([15]). By comparison with the experiments, best fitting parameters (such as the plasma frequency and scattering rate) were obtained and reported in the work of Kumar et al. [12] for each individual reflector. The fitted parameters obtained for the two films are not the same because of variation in the conditions of deposition and post treatment. There exists a large fraction of residual normal electrons at temperatures below T_c. The buffer layers have negligible effect to either the phase shift or the transmittance and reflectance.

The refractive index of Si depends on the frequency, increasing by about 0.1 percent from 10 to 100 cm^{-1} ([17]). Such small variation is negligible in the frequency region considered here; therefore, the refractive index of Si is assumed to be dependent only on temperature. The refractive index of Si changes from 3.42 at 300 K to 3.39 at 10 K as obtained by fitting the interference fringes in the transmittance and reflectance spectra of a bare Si substrate ([12,18]). The substrate thicknesses are $d_{\rm Si}=203.6$ μm and 204.3 μm for the two reflectors, respectively. Changes in $d_{\rm Si}$ due to thermal expansion are within 0.024 percent throughout the temperature range, which is negligibly small. The uncertainty in the refractive index and thickness of Si is approximately 0.5 percent. The surfaces are optically smooth with a root-mean-square roughness of a few nanometers. Because the wavelength is longer than 100 μm, the effect of surface roughness can be neglected.

For the sake of brevity, only the results at 300 K and 10 K are presented. The transmittance of the resonator is very sensitive to the optical path length introduced by the spacer. The thickness of the polyimide spacer measured with a micrometer was 132 μm. To obtain a good agreement with the measured fringes, in the computation, the cavity length was adjusted to 138 μm at 300 K and 134 μm at 10 K. This discrepancy may be due to the beryllium copper springs not being tight enough. Excessive tightening was avoided as it might break the samples. At low temperatures, there may be a decrease in the cavity length due to thermal contraction of the polyimide film (about 1–2 μm) and the effect of the beryllium copper springs. The cavity length is the only adjustable parameter in the calculation using Eq. (1) or (4).

Another important issue is the parallelism between the two reflecting surfaces. Only manual adjustments were done before the experiments to maintain the two reflectors as parallel as possible. Parallelism between the two reflecting surfaces also might have suffered from the uneven tightening of the springs. Equations from thin-film optics are strictly applicable to completely coherent

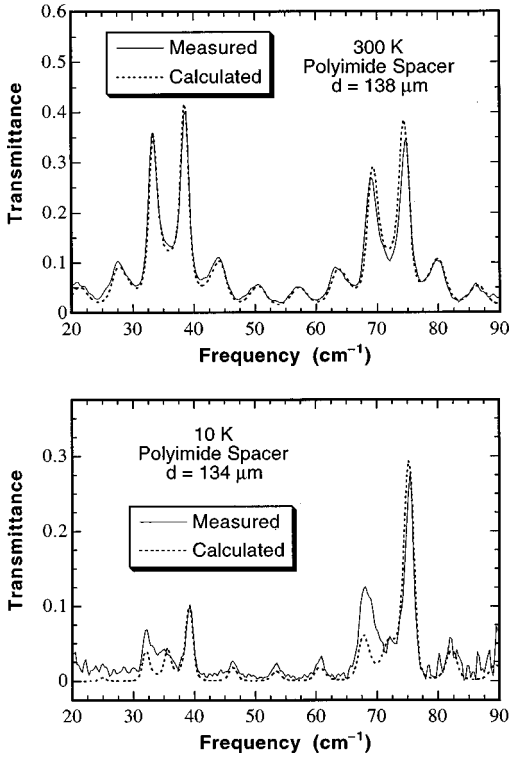

Fig. 4 Comparison between the measured and calculated transmittance, where *d* indicates the cavity length used in the calculation

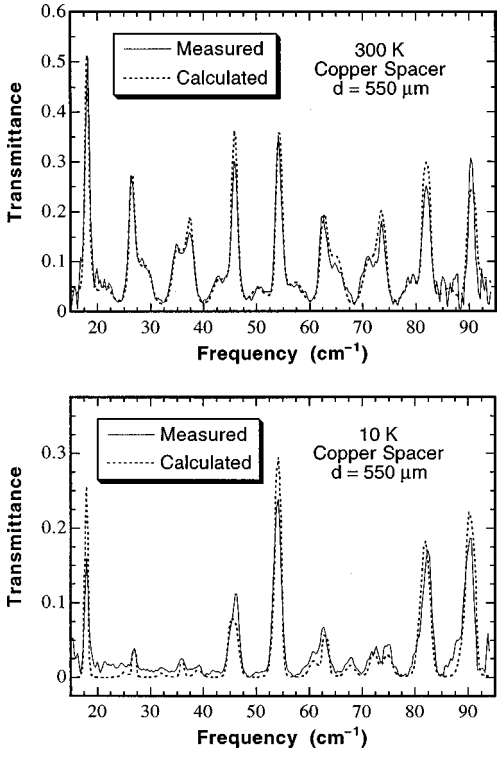

Fig. 5 Measured and calculated transmittance of the resonator with the copper spacer at 300 and 10 K

cases but nonparallelism can significantly reduce the fringe contrast and peak transmittance. The effect of partial coherence on the radiative properties of thin films were studied by many authors ([19–22]). The finite spectral resolution and beam divergence also reduce the coherence ([20]). In the experiments, the frequency interval between data points was 0.28 cm^{-1} and the spectral resolution was 0.56 cm^{-1}. The spatial incoherence caused by the nonparallelism (between the two films) and by the beam divergence (due to the finite solid angle) increases towards higher frequencies ([21]). Therefore, an empirical relation is introduced for the frequency-dependent effective resolution ($\delta\omega$):

$$\delta\omega = \sqrt{0.56^2 + (0.02\omega)^2}. \tag{6}$$

Equation (6) gives an effective resolution from about 0.6 to 2.1 cm^{-1} as ω changes from 10 to 100 cm^{-1}. In the computation, the transmittance is integral averaged from $\omega - \delta\omega/2$ to $\omega + \delta\omega/2$ for each point. Figure 4 shows the comparison between the measured transmittance and calculated transmittance which includes the effect of partial coherence. The measured and calculated values agree closely except for the spectra at 10 K in the regions from 30 to 37 cm^{-1} and from 65 to 72 cm^{-1}. The reason for this disagreement needs further investigation.

The measured and calculated transmittance at 300 K and 10 K for the resonator with the copper spacer is shown in Fig. 5. The main resonant peaks are located at approximately 9 cm^{-1} (which is below the cutoff frequency), 18 cm^{-1}, 27 cm^{-1}, etc. The interference in the Si substrates has a strong effect on the peak transmittance because $\mathcal{T}_{res}$ changes drastically with frequency, which will be discussed in the following section. The measured peak transmittance is 0.51 at 300 K and 0.16 at 10 K for the second-order resonance. The FWHM bandwidth for this transmittance peak is 1.1 cm^{-1} and 0.9 cm^{-1} at 300 K and 10 K, respectively.

To demonstrate the effect of partial coherence, the transmittance calculated directly from thin-film optics (complete coherence) with a frequency interval of 0.05 cm^{-1} is compared with that calculated considering partial coherence in Fig. 6. The effect of partial coherence is particularly large for sharp transmittance peaks. It is not surprising that the agreement in Fig. 5 is not as good as that in Fig. 4. Notice that the bandwidth of the transmittance peak broadens due to partial coherence. Higher spectral

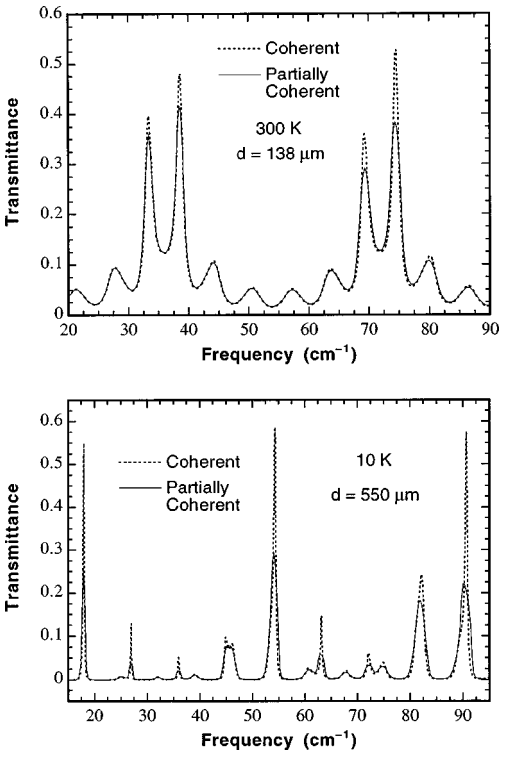

Fig. 6 The effect of partial coherence on the resonant transmittance

resolution with improved alignment between the two reflecting surfaces should be used in future measurements.

5 Discussion

Optimization of the Resonant Transmittance. The radiative properties of individual reflectors, which are related to the interface effects in the substrates, strongly influence the transmittance characteristics of the resonator. The resonant transmittance $\mathcal{T}_{res}$, determined from Eq. (3), depends entirely on the two reflectors but not on the cavity length. Figure 7 plots the calculated T_1, R_1 and ϕ_1 of the first reflector, together with $\mathcal{T}_{res}$ at 300 K and 10 K for completely coherent situation. The properties of the second reflector are very similar to these of the first one since the substrate thickness is nearly the same. All spectra oscillate due to interference in the substrate with a period (free spectral range) of $\Delta\omega_{Si}=(2n_{Si}d_{Si})^{-1}$, where d_{Si} is the thickness and n_{Si} the refractive index of Si. In the normal sate, the fringe contrast in the reflectance is much larger than that in the transmittance. Therefore, the maxima of both $\mathcal{T}_{res}$ and R_1 are located at the same frequencies, given by

$$\omega_{m_{Si}}=\frac{2m_{Si}+1}{4n_{Si}d_{Si}}, \tag{7}$$

where m_{Si} is the order of resonance in the Si substrate. At frequencies equal to $\omega_{m_{Si}}$, ϕ_1 is approximately zero. In order to achieve the maximum peak transmittance, the particular resonance in the cavity must be coincident with one of the resonances in the substrates. Since $\phi_1\approx\phi_2\approx 0$ at the substrate resonance, Eq. (4) suggests that β must equal $2\pi m$, corresponding to the main resonant frequencies $\omega_m=m/2d$. By equating ω_m and $\omega_{m,Si}$, we have

$$d=\frac{2n_{Si}m}{2m_{Si}+1}d_{Si} \tag{8}$$

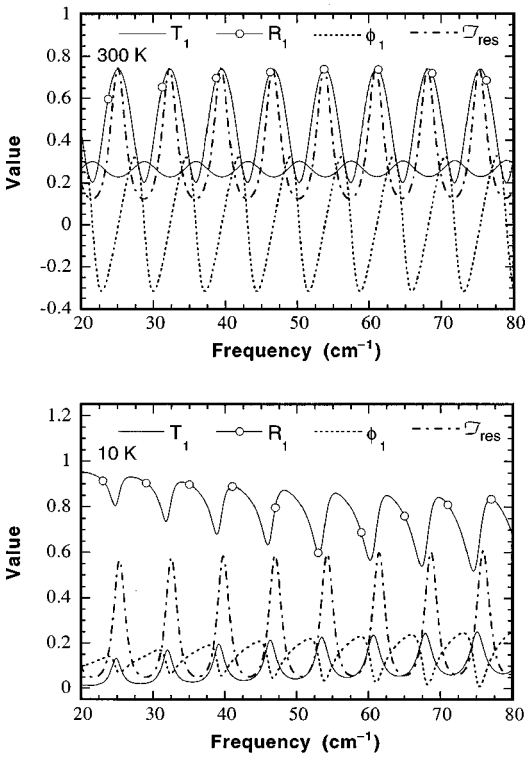

Fig. 7 Calculated transmittance *T*, reflectance *R*, and phase shift upon reflection ϕ for the first reflector, together with $\mathcal{T}_{res}$

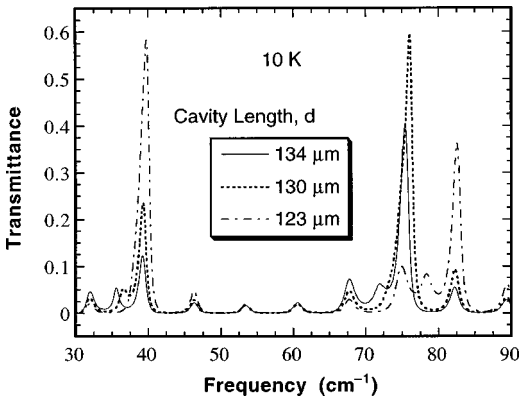

Fig. 8 The effect of cavity length on the peak transmittance for the first and second-order resonance

which is a criterion for obtaining maximum resonant transmittance.

In the superconducting state, Fig. 7(*b*) shows that ϕ_1 is always greater than zero and the behavior of T_1 and R_1 are quite different from those in the normal state. The maxima of $\mathcal{T}_{res}$, however, are still located near $\omega_{m_{Si}}$, where ϕ_1 is close to zero. Therefore, Eq. (8) provides a good approximation for getting the best performance. The actual value of optimum d may be slightly different from that given by Eq. (8).

Equation (8) was originally obtained by Malone et al. [9]. They adjusted the substrate thickness in the computation to predict the maximum resonant transmittance. Here, we have provided detailed derivations of Eq. (8) by analyzing the resonator transmittance equation and the properties of each individual reflector. In practice, it is often easier to adjust the cavity length. In our experiments, the value of d was chosen at random and was kept constant. In order to show that HTSC films on transparent substrates are indeed good candidates for far-infrared resonators, the cavity length d is varied to compute the optimal characteristics of the resonator.

The peak transmittance is optimized for the first and second-order of the cavity resonance (i.e., $m=1,2$) for 10 K. The value of m_{Si} is chosen so that the value of d lies in the close vicinity of 134 μm, the value obtained from the experiment. Using $n_{Si}=3.39$ and $d_{Si}=204$ μm, which is the average thickness of the two substrates, Eq. (8) gives the values of d that yield the maximum transmittance to be 126 μm ($m_{Si}=5$) and 133 μm ($m_{Si}=10$), respectively, for the first and second-order resonance. The actual optimized cavity lengths are $d=123$ μm and 130 μm. Figure 8 compares the calculated transmittance for the cavity lengths optimized for the first and second-order resonance with that obtained from the experiment. All three cases are assumed to be completely coherent. The optimized peak transmittance is near 0.6, which is 400 percent higher than the peak transmittance for the first-order resonance obtained from the experiment. Another important feature in the optimized situation is that the sidebands have been substantially reduced, which is the advantage of using thin Si substrates as compared with the 0.5 mm thick Si substrates used by Pechen et al. [8]. The value F calculated from Eq. (2) also oscillates. Because $\mathcal{T}_{res}$ and ϕ_1 change drastically with frequency, the value of F calculated from Eq. (2) is not an indicator of the finesse anymore. The finesse is calculated by dividing the free spectral range by the FWHM bandwidth.

The above method can be applied to optimize the performance for various ranges of d and at different temperatures. These calculations demonstrate that HTSC materials are promising candidates for constructing far-infrared resonators. The performance of the resonator, however, is a strong function of the cavity length. Therefore, a mechanism that can adjust the cavity length within a

few micrometers during the measurement is required and is currently under development to achieve the optimal performance.

The Effect of the YBCO Film. The YBCO film thickness affects the transmittance, reflectance, and absorptance of the individual reflectors, which in turn affect the transmittance characteristics of the resonator. Increasing the film thickness will decrease the transmittance of the film/substrate composite, yielding a reduction in the peak transmittance of the resonator as can be seen from Eq. (3). However, increasing the film thickness will increase the reflectance of the film/substrate composite, which in turn will improve the finesse, see Eq. (2).

The effect of the YBCO film thickness is studied by a computer simulation, in which the film thickness is varied on one or both reflectors, under conditions that facilitate the maximum possible first-order resonant transmittance. Only a brief summary is given here. As the YBCO thickness decreases, the peak resonant transmittance increases and reaches 1 for zero thickness (i.e., only Si substrates). The height of the sidebands also increases as the YBCO film thickness decreases. The bandwidth of the transmittance peaks shows a decreasing trend with the increase in the YBCO film thickness, indicating that the finesse is increasing. Hence, in the resonator design, a compromise must be made between high resonant transmittance and high finesse with suppressed sidebands. The thickness of the YBCO film should generally be equal to or less than 50 nm in order to have acceptable resonant transmittance. The quality of the YBCO film also affects the resonator's performance. High-quality films with little residual absorption in the superconducting state will improve the peak transmittance and finesse.

6 Conclusions and Future Work

We have measured the transmittance of Fabry-Perot resonators using YBCO films on Si substrates as the reflecting surfaces in the far-infrared region at temperatures between 10 and 300 K. The sidebands observed in previous studies have been suppressed by the use of thin substrates. The resonant transmittance decreases with temperature in the normal state but can increase in the superconducting state as the temperature goes down. The calculated transmittance, considering partial coherence, is in good agreement with the experimental data. An optimization analysis was performed to predict the maximum resonant transmittance by examining the interference effects in the cavity and substrates. The transmittance characteristics of the resonator are very sensitive to the thickness of each layer that forms the resonator. The maximum resonant transmittance is obtained when a particular resonance in the cavity is coincident with one of the substrate resonances. An increase in the YBCO film thickness will improve the finesse but reduce the peak transmittance.

This work demonstrates the potential of using YBCO thin films on thin Si substrates to construct Fabry-Perot resonators and can serve as the basis for the future design of such resonators. We are developing a mechanism that will improve the alignment between the two reflectors and will allow fine-tuning of the cavity length during the measurement. A higher spectra resolution should be used to discern sharp transmittance peaks. The quality of the YBCO film should be improved with reduced residual absorption to achieve a better performance.

Acknowledgments

The authors would like to thank Dr. Leila Vale and Dr. David Rudman of the National Institute of Standards and Technology for providing the superconducting film samples. This work has been supported by the National Science Foundation (NSF) through grant CTS-9812027. Z.M.Z. is also grateful to the NSF support through a PECASE award (CTS-9875441).

Nomenclature

A = absorptance
d = cavity length, cm
d_{Si} = thickness of the Si substrate, cm
F = finesse
m = order of resonance (or interference fringe)
n = refractive index
R = reflectance of the film/substrate composite
T = transmittance of the film/substrate composite
T_c = critical temperature, K
$\mathcal{T}$ = transmittance of the resonator
$\mathcal{T}_{res}$ = resonant transmittance
β = phase shift inside the cavity, rad
ϕ = phase shift upon reflection, rad
ψ = $\beta+\phi_1+\phi_2$, Eq. (4)
ω = frequency, cm^{-1} ($1\ cm^{-1}=2.9979\times10^{10}$ Hz)
ω_m = resonance frequency, cm^{-1}
$\Delta\omega$ = fringe separation (or free spectral range), cm^{-1}
$\delta\omega$ = spectral resolution, cm^{-1}

Subscripts

1 = first film
2 = second film
Si = silicon

References

[1] Brodbeck, R., Pepe, F. A., Tognina, C., Bhend, D., Zimmerman, E., and Kneubuhl, F. K., 1998, ''Balloon-Borne Far-Infrared Fabry-Perot Spectrometers for Astrophysical Observations,'' Infrared Physics and Technology, **39**, pp. 393–414.
[2] Vaughan, J. M., 1989, *The Fabry-Perot Interferometer*, Adam Hilger Publishers, Philadelphia, PA.
[3] Komm, D. S., Blanken, R. A., and Brossier, P., 1975, ''Fast-Scanning Far-Infrared Fabry-Perot Interferometer,'' Appl. Opt., **14**, pp. 460–464.
[4] Renk, K. F., and Genzel, L., 1962, ''Interference Filters and Fabry-Perot Interferometers for the Far Infrared,'' Appl. Opt., **1**, pp. 643–648.
[5] Belland, P., and Lecullier, J. C., 1980, ''Scanning Fabry-Perot Interferometer: Performance and Optimum Use in the Far Infrared Range,'' Appl. Opt., **19**, pp. 1946–1952.
[6] Renk, K. F., Betz, J., Schützmann, J., Prückl, A., Brunner, B., and Lengfellner, H., 1990, ''Use of High T_c Superconductors for Far-Infrared Fabry-Perot Resonators,'' Appl. Phys. Lett., **57**, pp. 2148–2149.
[7] Wiese, P., Riederer, X., Schützmann, J., Gorshunov, B., Betz, J., and Renk, K. F., 1992, ''Far-Infrared Fabry Perot Filter of High Transmission With High-T_c Superconductor Reflectors,'' Int. J. Infrared Millim. Waves, **13**, pp. 65–70.
[8] Pechen, E. V., Vent, S., Brunner, B., Prückl, A., Lipp, S., Linder, G., Alexandrov, O., Schützmann, J., and Renk, K. F., 1992, ''Far-Infrared Fabry-Perot Resonator With High T_c $YBa_2Cu_3O_{7-\delta}$ Films on Silicon Plates,'' Appl. Phys. Lett., **61**, pp. 1980–1982.
[9] Malone, C. G., Zhang, Z. M., Flik, M. I., and Cravalho, E. G., 1993, ''Optimized Design of Far-Infrared Fabry-Perot Resonators Fabricated From $YBa_2Cu_3O_7$,'' IEEE Trans. Appl. Supercond., **3**, pp. 2852–2855.
[10] Kumar, A. R., and Zhang, Z. M., 1999, ''Far-Infrared Spectroscopy of High-Temperature Superconducting Films on Silicon Substrates,'' *Recent Research Developments in Applied Spectroscopy*, Vol. 2, S. G. Pandalai, ed., Research Signpost, India, pp. 99–112.
[11] Rice, J. P., Grossman, E. N., and Rudman, D. A., 1994, ''Antenna-Coupled High-T_c Air-Bridge Microbolometer on Silicon,'' Appl. Phys. Lett., **65**, pp. 773–775.
[12] Kumar, A. R., Zhang, Z. M., Boychev, V. B., Tanner, D. B., Vale, L. R., and Rudman, D. A., 1999, ''Far-Infrared Transmittance and Reflectance of $YBa_2Cu_3O_{7-\delta}$ Films on Si Substrates,'' ASME J. Heat Transfer, **121**, pp. 844–851.
[13] Sanderson, R. B., and Scott, H. E., 1971, ''High Resolution Far Infrared Interferometer,'' Appl. Opt., **10**, pp. 1097–1102.
[14] Kumar, A. R., Zhang, Z. M., Boychev, V. B., and Tanner, D. B., 1999, ''Temperature-Dependent Far-Infrared Absorptance of Thin $YBa_2Cu_3O_{7-\delta}$ Films in the Normal State,'' Microscale Thermophys. Eng., **3**, pp. 5–15.
[15] Tanner, D. B., and Timusk, T., 1992, ''Optical Properties of High-Temperature Superconductors,'' *Physical Properties of High-Temperature Superconductors*, Vol. 3, D. M. Ginsberg, ed., World Scientific Publishing, Singapore, pp. 363–469.
[16] Zhang, Z. M., Kumar, A. R., Boychev, V. B., Tanner, D. B., Vale, L. R., and Rudman, D. A., 1998, ''Back-Side Reflectance of High T_c Superconducting Thin Films in the Far Infrared,'' Appl. Phys. Lett., **73**, pp. 1907–1909.

[17] Loewenstein, E. V., Smith, D. R., and Morgan, R. L., 1973, ''Optical Constants of Far-Infrared Materials, 2: Crystalline Solids,'' Appl. Opt., **12**, pp. 398–406.
[18] Kumar, A. R., 1999, ''Far-Infrared Radiative Properties of Superconducting YBCO Films Deposited on Silicon Substrates,'' Ph.D. Dissertation, University of Florida, Gainesville, FL.
[19] Chen, G., and Tien, C. L., 1992, ''Partial Coherence Theory of Thin Film Radiative Properties,'' ASME J. Heat Transfer, **114**, pp. 636–643.
[20] Zhang, Z. M., 1994, ''Optical Properties of Layered Structures for Partially Coherent Radiation,'' *Proc. Tenth Intl. Heat Transfer Conf.*, Vol. 2, G. F. Hewitt, ed., Taylor and Francis, London, pp. 177–182.
[21] Grossman, E. N., and McDonald, D. G., 1995, ''Partially Coherent Transmittance of Dielectric Lamellae,'' Opt. Eng., **34**, pp. 1289–1295.
[22] Anderson, C. F., and Bayazitoglu, Y., 1996, ''Radiative Properties of Films Using Partial Coherence Theory,'' J. Thermophys. Heat Transfer, **10**, pp. 26–32.